Non-Markovian Mpemba effect in mean-field systems

Zhen-Yu Yang[*] and Ji-Xuan Hou [†]

School of Physics, Southeast University, Nanjing 211189, China

Under certain conditions, a counterintuitive behavior—an initially hotter sample freezes faster when quenched to a cold bath than an identical system initialled at a lower temperature—is known as the Mpemba effect (ME). Here we identify the existence of the ME in mean-field systems (MFS). Specifically, the thermal contact between MFS and a large thermal reservoir is built up using the microcanonical Monte Carlo algorithm. The simulation results unambiguously demonstrate that an initial hotter system undergoes the paramagnetic-ferromagnetic phase transition faster than the initial cooler one. The ME here originates from the back-reaction of the MFS system on the reservoir, which is thus an embodiment of non-Markovianness in relaxation. In addition, we confirm that the ME survives in the thermodynamic limit. And the significance of reservoir size is also explored: A smaller heat reservoir facilitates the overall relaxation process. In general, this work establishes a theoretical non-Markovian ME framework, which may shed light on widening the understanding of the mechanism behind the ME in other substances, including water.

I. INTRODUCTION

Considering putting two beakers of water with different initial temperatures to a cold bath, intuitively, one may expect that less time is needed for the colder one to freeze. Surprisingly, it has been observed that this is not always the case [1]. The records about this counterintuitive phenomenon can be traced back to antiquity like Aristotle, Roger Bacon, Francis Bacon, and Descartes [2,3]. Nowadays, this paradoxical behavior is named the "the Mpemba effect" (ME). It refers to the effect that occurs when two samples of the same substance identical in all macroscopic states except for their initial temperatures, the initially high-temperature substance relaxes faster when quenched to lower temperatures. However, there is no agreement on the exact underlying mechanism of the Mpemba effect in the water, and even its existence has been recently called into question after careful analysis of the experimental data by Burridge *et al.* [4]. Several possible postulations were proposed during the past several decades pointing to evaporation and convection [5–10], dissolved gases [11–13], the relationship between intramolecular polar-covalent bonds (O-H), and intermolecular hydrogen bonds (O:H) [14], etc.

This nonequilibrium process [15,16] is not only specific to water. Recently, a renewed theoretical interest in the effect emerged, after a rather general statistical-physics framework has been put forward: the "Mpemba-like" effect. And it has been reported that the effect may occur in many Markov processes ("the Markovian Mpemba effect") where hot systems cool faster than colder ones (or vice versa, cold systems heat faster than hotter ones). Typical systems include nanotube resonators [17], spin glasses [18], granular fluids [19], and Ising model [16]. The underlying mechanisms of the Markovian ME vary. For example, the ME in granular fluids and spin glasses originate from the additional factors that control the temperature relaxation [18,19]. While in the Ising model and three-state system, Klich reported that systems with different carefully chosen initial preparations quench along different trajectories [16]. However, fewer studies have identified that the existence of Mpemba-like effect in a non-Markov process. Meanwhile, the studies have to date only regarded the quenching rate and thus lacked a description of the effect in a system undergoing a phase transition akin to the freezing of water.

In this work, we identified the occurrence of the ME in mean-field systems (MFS) undergoing a paramagnetic-ferromagnetic phase transition. Completely distinct from the previous studies, the mechanism of the ME here is an embodiment of non-Markovianness in relaxation. In addition, this work not only provides another interpretation of a prototypical system where the ME occurs but also is the first study to examine the effect across a phase transition, which brings such studies closer to the original effect in freezing water.

II. MEAN-FIELD MODEL

We consider a mean-field model composed of N fermions and placed in a staggered magnetic field. The Hamiltonian reads [20–23]

$$H = -\sum_{i=1}^{\frac{N}{2}} \frac{K}{2} S_i + \sum_{i=\frac{N}{2}+1}^{N} \frac{K}{2} S_i$$
$$- \frac{J}{2N}\left(\sum_{i=1}^{N} S_i\right)^2 - \frac{I}{4N^3}\left[\left(\sum_{i=1}^{N} S_i\right)^2\right]^2, \quad (1)$$

[*]Also at Department of Radiation Oncology, Duke University Medical Center, Durham, NC, USA.
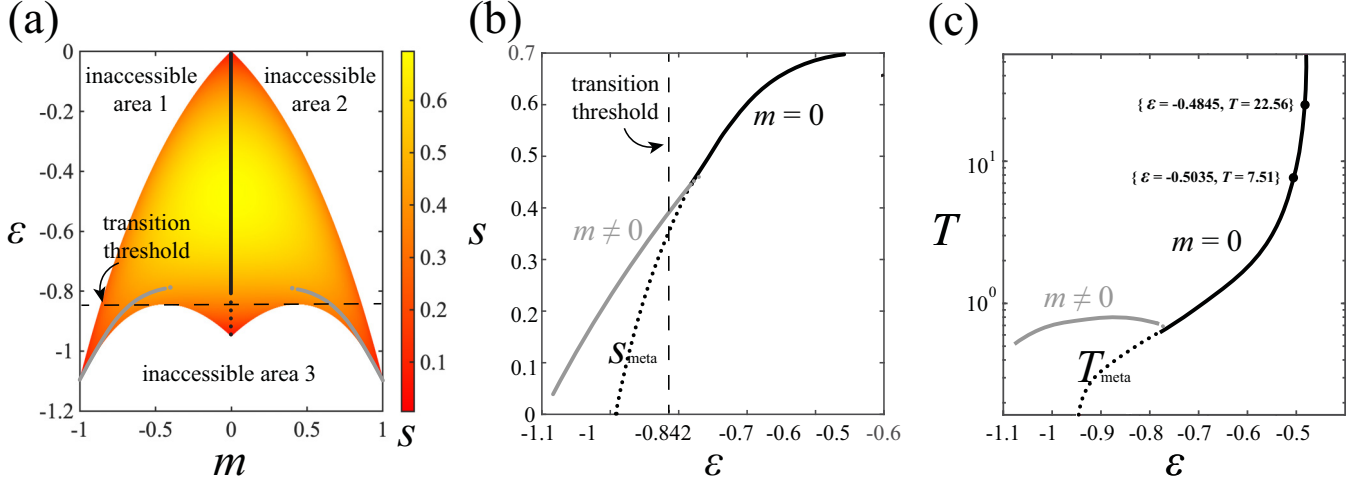[†]jxhou@seu.edu.cn

FIG. 1. Thermodynamic properties of our mean-field system. (a) The entropy diagram of our mean-field model in the m-ε plane, where the blank regions are inaccessible. The equilibrium states and metastable states are highlighted by the solid and dotted lines, respectively. The black and gray of those lines indicate the nonmagnetized state and the ferromagnetic state, respectively. The dashed line is the dividing of spontaneously evolving region and nonspontaneously evolving region. (b) The corresponding final entropy s as a function of energy ε. (c) The corresponding caloric curve.

where $S_i = \pm 1$. The first two terms on the right-hand side of Eq. (1) represent the interaction with a staggered magnetic field, and K is the intensity of the magnetic field. The third and the fourth terms are the long-range mean-field coupling terms, which are common in magnetic materials with easy magnetic axes. It is worth mentioning that many novel features can be encountered when manipulating the values of I, J, and K [20–23]. Here we choose the setting $\{K = -0.95, \ J = 1, \ I = 0.5\}$ for the following discussion. The simplicity of the spin chain model makes it an ideal and apt benchmark for other, more complex, MFS.

The main thermodynamic properties of this model, including entropy, energy, temperature, heat capacity, and phase diagram, can be fully solved via the microcanonical approach. Suppose N_L^+ and N_L^- are the numbers of upward and downward spins in the left part of the system. Correspondingly, N_R^+ and N_R^- are upward and downward spins on the right side. The compliance number U and the magnetization of the system M can be defined as $U \equiv N_L^- + N_R^+$ and $M \equiv 2(N_R^+ - N_L^-)$, respectively. The magnetization per spin and diamagnetic susceptibility per spin thus are $m \equiv M/N$ and $u \equiv U/N$. Then the entropy and the energy per spin can be obtained as

$$
s(\varepsilon, m) = -\frac{1}{2}\left(u + \frac{m}{2}\right)\ln\left(u + \frac{m}{2}\right)
$$
$$
- \frac{1}{2}\left(1 - u - \frac{m}{2}\right)\ln\left(1 - u - \frac{m}{2}\right)
$$
$$
- \frac{1}{2}\left(u - \frac{m}{2}\right)\ln\left(u - \frac{m}{2}\right)
$$
$$
- \frac{1}{2}\left(1 - u + \frac{m}{2}\right)\ln\left(1 - u + \frac{m}{2}\right), \quad (2)
$$

and

$$
\varepsilon = Ku - \frac{J}{2}m^2 - \frac{I}{4}m^4, \quad (3)
$$

respectively. See the Supplemental Material [24] for the detailed derivation. Accordingly, the temperature is

$$
T = \frac{1}{\partial s(\varepsilon)/\partial \varepsilon}. \quad (4)
$$

Figure 1(a) is the entropy s diagram in the m-ε plane, where the colorful regime is accessible to the MFS. While the existence of inaccessible region (i.e., blank region) causes the magnetization of this system cannot vary within the interval $[-1, +1]$ for any given energy ε. The ergodicity of the MFS is thus broken. In the thermodynamic limit $N \to \infty$, the final entropy $s(\varepsilon)$ for any given energy ε is obtained by maximizing $s(m, \varepsilon)$ with respect to the magnetization m. And the spontaneous magnetization $m(\varepsilon)$ can be obtained at the same time. Alternatively, the global maximum of $s(\varepsilon)$ at any given energy corresponds to the equilibrium state, which is highlighted as the thick solid black and gray lines in Fig. 1(a). Moreover, the local maximum entropy values, marked as the dotted black and gray lines, can be regarded as the metastable states. Following the solid lines in Fig. 1(a), as the energy ε decreases, the system evolves from the paramagnetic state ($m = 0$, solid black line) to ferromagnetic state ($m \neq 0$, solid gray lines) through a first-order phase transition at $\varepsilon = -0.787$. It is useful to introduce an energy threshold, named the "transition threshold," which is corresponding to the topmost boundary of the inaccessible area 3 in Fig. 1(a). Here the transition threshold is -0.842. Naturally, for the MFS in region $-0.842 < \varepsilon < -0.787$, it is possible to evolve from the paramagnetic state to the ferromagnetic state spontaneously. Conversely, an isolated nonmagnetized MFS with $\varepsilon < -0.842$ can only be trapped in this the metastable state permanently since the existence of the inaccessible region creates an insurmountable energy barrier. See the Supplemental Material [24] for simulation. Figures 1(b) and 1(c) shows the corresponding final entropy evolution (s–ε) track and caloric (T–ε) curve, respectively.
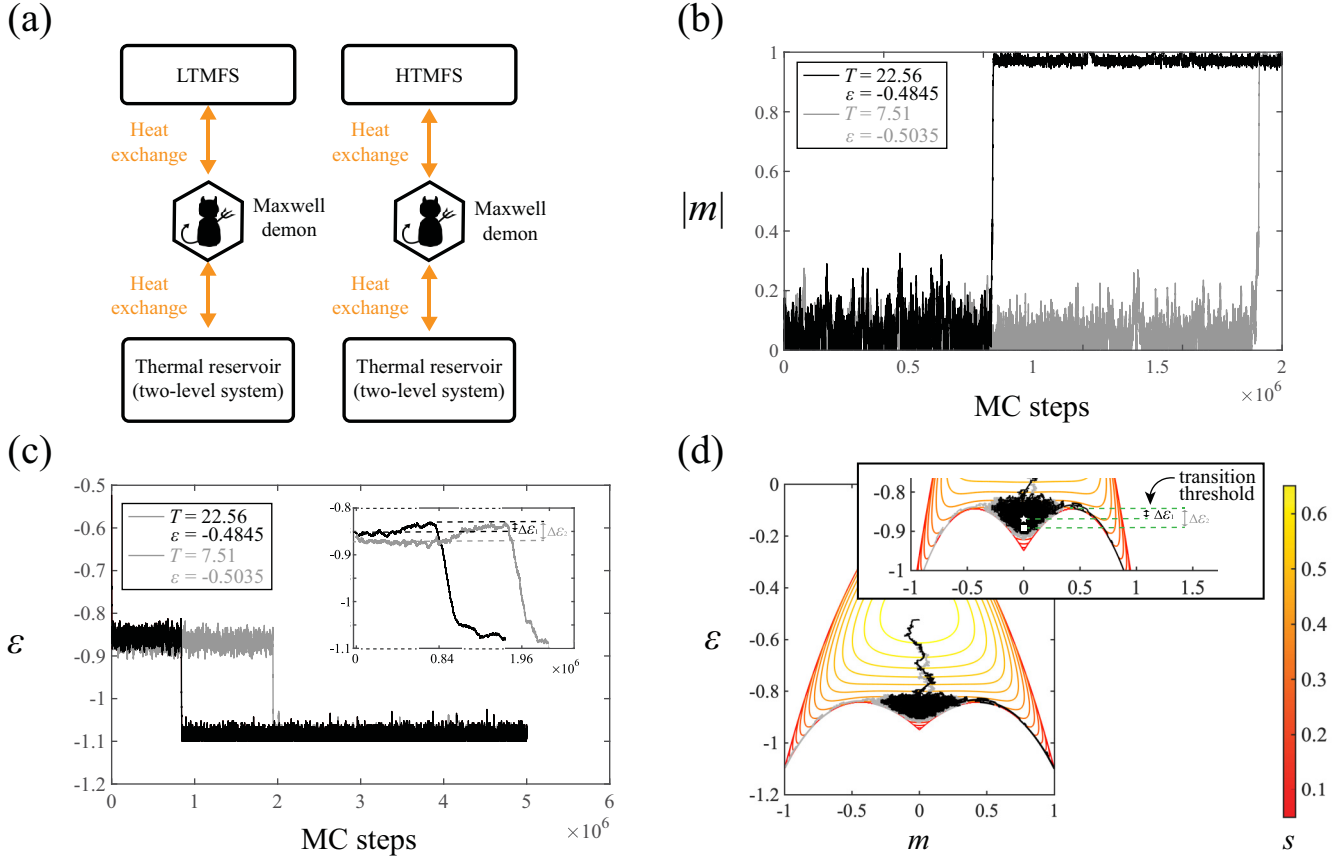
FIG. 2. The microcanonical Monte Carlo simulation of the heat exchange between the thermal reservoir and two MFSs with different initial temperatures. (a) The schematic diagram of the simulation. (b) The simulation result of (absolute value of) magnetization evolution, where the initial hotter and cooler system are represented by the black and gray lines, respectively. (c) The simulation result of energy evolution. (c) Inset: The energy changing near the phase transition point. (d) The evolution paths for two MFSs in the m-ε plane. (d) Inset: The illustration of energy barriers $\Delta\varepsilon_1$ and $\Delta\varepsilon_2$ for HTMFS and LTMFS, respectively. And white star and square markers represent the corresponding metastable states.

III. MONTE CARLO SIMULATION AND MPEMBA EFFECT

We investigate the ME by simulating the quenching processes of two MFSs initialled at different temperatures. Specifically, microcanonical Monte Carlo (MC) numerical simulations proposed by Creutz [28] is performed to examine the thermal contact between a thermal reservoir and two MFSs with different initial temperatures. To simplify the calculation, we adopt the noninteracting two-level thermal system with the energy difference ε_0 as the thermal reservoir. Without loss of generality, ε_0 is set to be unity. The numbers of the spins of MFS and the reservoir are simply set as $N = 400$ and $N_{\text{bath}} = 20N$. By carefully manipulating the ratio of the spin up and spin down, we can initialize the MFS to any temperature. Here we choose the temperature and corresponding energy configurations $\{T = 22.56, \varepsilon = -0.4845\}$ and $\{T = 7.51, \varepsilon = -0.5035\}$ to represent the initial "hotter" and "cooler" system, respectively, and we refer to them as "HTMFS" and "LTMFS," respectively. In addition, the two-level bath is initially set to 0K, which suggests that all the spins of the reservoir stay at the lowest energy state.

Figure 2(a) shows the sketch of the details of our simulation process [29]. The thermal contact is achieved by an addi-

tional degree of freedom, named as "demon." Such a demon is introduced to carry a small amount of energy ε_D, which must always be non-negative. Moreover, ε_D is initially set as 0 and without upper energy limit. In each MC step, we randomly select a spin in the system MFS or the reservoir based on the ratio of N to N_{bath}, and flip it. The change of the energy of the full system is ΔE. If $\Delta E < 0$, then the trial movement is accepted, and the energy of the "demon" is increased by $|\Delta E|$. If $0 \leqslant \Delta E \leqslant \varepsilon_D$, then the trial move is also accepted but energy of the "demon" is decreased by $|\Delta E|$. Otherwise, the trial move is rejected, and the energy of the demon does not change. Consequently, the heat exchange between the MFS and the thermal reservoir can be conducted with the help of the demon. The probability of the thermal contact between demon-MFS and demon-reservoir only depends on $N : N_{\text{bath}}$.

The simulation results of the absolute values of magnetization $|m|$ and energy ε of the MFS changing with the number of the MC steps are plotted in Figs. 2(b) and 2(c), respectively. The black lines represent the simulation results of the HTMFS ($T = 22.56$, $\varepsilon = -0.4845$), while the gray lines are on behalf of the LTMFS ($T = 7.51$, $\varepsilon = -0.5035$). The inset in Fig. 2(c) details the energy changes near the phase transition point. The sudden jump of $|m|$ declares the occurrence of the first-order phase transition from the paramagnetic to the

ferromagnetic state. The abscissa MC steps are proportional to the evolution of time [30,31]. In this diagram, the emerge of the ME is clearly demonstrated as less relaxation time is needed for the HTMFS system.

To visualize the underlying mechanism of the occurrence of the ME here, the behaviors of MFS as a function of time is investigated. The evolution paths of m and ε can be mapped onto the theoretic entropy map, shown in Fig. 2(d) (see videos 1 and 2 in the Supplemental Material [24] for the animations of the evolution processes). By exchanging the heat with the thermal bath, two MFSs first cool rapidly alone the paramagnetic line. The finiteness of the system leads to the non-Markovianity of the dynamic, where the back-reaction from the MFS heats the original 0K reservoir during this process. Then the MFS reaches the temporary equilibrium, i.e., metastable state, with the heated reservoir. The locus of the metastable states for HTMFS and LTMFS are marked as the white star and square markers in Fig. 2(d), respectively. As discussed, the free-energy barrier caused by the inaccessibility prevents spontaneous evolution from such a metastable state to equilibrium. However, with the help of the thermal reservoir, the MFS may draw sufficient energy from the reservoir through a thermal fluctuation and cross the transition threshold to the final ferromagnetic state after a certain period of time. According to Mukamel *et al.* [30], the lifetime τ of the metastable state satisfies the Arrhenius law as

$$\tau \sim \exp\left(N\Delta\varepsilon\right). \tag{5}$$

The initially hotter system dumps more energy to the reservoir, and consequently heats it up more, than the initially colder system. Thus, when the two systems are trapped in the metastable state, the system initialled at a hotter state is effectively coupled to a hotter reservoir, reducing the energy barrier to the final ferromagnetic state. That is, the energy barriers for HTMFS $\Delta\varepsilon_1$ is smaller than that of LTMFS $\Delta\varepsilon_2$. As a consequences, the non-Markovian ME ($\tau_1 < \tau_2$) emerges.

Note that the precise amount of the energy barrier can be obtained by calculating the exact location of the metastable state. The interaction energy ε_{int} between these two subsystems can be neglected under the weak-coupling condition ($\varepsilon_{\text{int}} \ll \varepsilon$, $\varepsilon_{\text{int}} \ll \varepsilon_{\text{bath}}$), and the full system thus remains isolated. Therefore, the total energy equals to the sum of the energies of two subsystems, i.e., $\varepsilon_{\text{full}} = \alpha\varepsilon + (1-\alpha)\varepsilon_{\text{bath}}$, where $\alpha = N/(N + N_{\text{bath}})$. The entropy per spin of the full system becomes $s_{\text{full}}(\varepsilon, \varepsilon_{\text{bath}}) = \alpha s(\varepsilon) + (1-\alpha)s_{\text{bath}}$.

According to the Eqs. (2) and (3), the entropy of the MFS that trapped in the metastable states ($m = 0$) can simplified as

$$s(\varepsilon) = -\frac{\varepsilon}{K}\ln\left(\frac{\varepsilon}{K}\right)$$
$$-\left(1 - \frac{\varepsilon}{K}\right)\ln\left(1 - \frac{\varepsilon}{K}\right).$$

It is well known that the entropy the two-level system expresses as

$$s_{\text{bath}}(\varepsilon_{\text{bath}}) = \ln 2 - \frac{1}{2}(1 + \varepsilon_{\text{bath}})\ln(1 + \varepsilon_{\text{bath}})$$
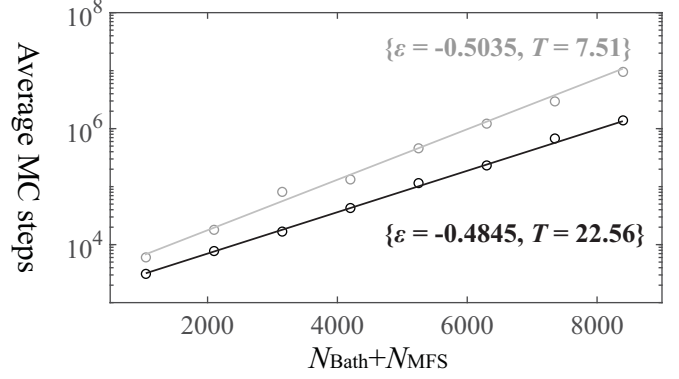$$-\frac{1}{2}(1 - \varepsilon_{\text{bath}})\ln(1 - \varepsilon_{\text{bath}}).$$

FIG. 3. The average lifetime of the metastable state, shown in log scale, as a function of the full system size. The black and gray circles represent the transition time of the MFSs initialled at $\{T = 22.56, \varepsilon = -0.4845\}$ and $\{T = 7.51, \varepsilon = -0.5035\}$, respectively. Two solid lines are the guides to the eye. The ratio $\alpha = N/(N + N_{\text{bath}}) = 1/21$.

Based on the second law of thermodynamics, the equilibrium state is the state in which the total entropy reaches its maximum. Thus the total entropy per spin is

$$s_{\text{full}}(\varepsilon_{\text{full}}) = \max_{\varepsilon} s_{\text{full}}(\varepsilon, \varepsilon_{\text{full}})$$
$$= \max_{\varepsilon}\left[\alpha s(\varepsilon) + (1 + \alpha)s_{\text{bath}}\left(\frac{\varepsilon_{\text{full}} - \alpha\varepsilon}{1 - \alpha}\right)\right]. \tag{6}$$

By solving the optimization Eq. (6), the values of energy, entropy, and temperature of each subsystem can be found. Therefore, when the initial energy of the full system and the size of each subsystem are given, the amount of the energy barrier can be obtained.

Coupling such a MFS to the reservoir is tricky [32]. According to Eq. (5), the lifetime τ of the metastable state scales exponentially with the number of particles in the system, indicating that the system can be trapped in the out-of-equilibrium metastable for sufficiently long time and thus cannot relax to the equilibrium [33]. Figure 3 illustrated the measured metastable state lifetime τ (or the transition time) as a function of the full system size, where the black and gray circles represent the average MC steps measured by 150 independent simulations of the initial hotter and cooler system, respectively. Two solid lines are a guide to the eye. Here we fix the ratio $\alpha = 1/21$, and the initial hotter and cooler systems inherit the configurations $\{T = 22.56, \varepsilon = -0.4845\}$ and $\{T = 7.51, \varepsilon = -0.5035\}$ for consistency. Apparently, the rate of increase of the transition time vary for systems with different initial temperatures, and the hotter system can always accomplish the phase transition faster than the cooler one. That is, the ME survives in the thermodynamic limit.

Another related issue is the impact of heat reservoir size on ME. Figure 4 demonstrates the relationships between average metastable state lifetime τ and energy barrier $\Delta\varepsilon$ versus the initial temperature T when $N_{\text{bath}}/N = 15$ and $= 20$. Here we keep $N = 400$. τ is again measured by 150 independent MC simulations and plotted as discrete yellow circle markers (mean values) with vertical error bars. The $\Delta\varepsilon$, obtained by theoretically solving Eq. (6), is shown as continuous solid
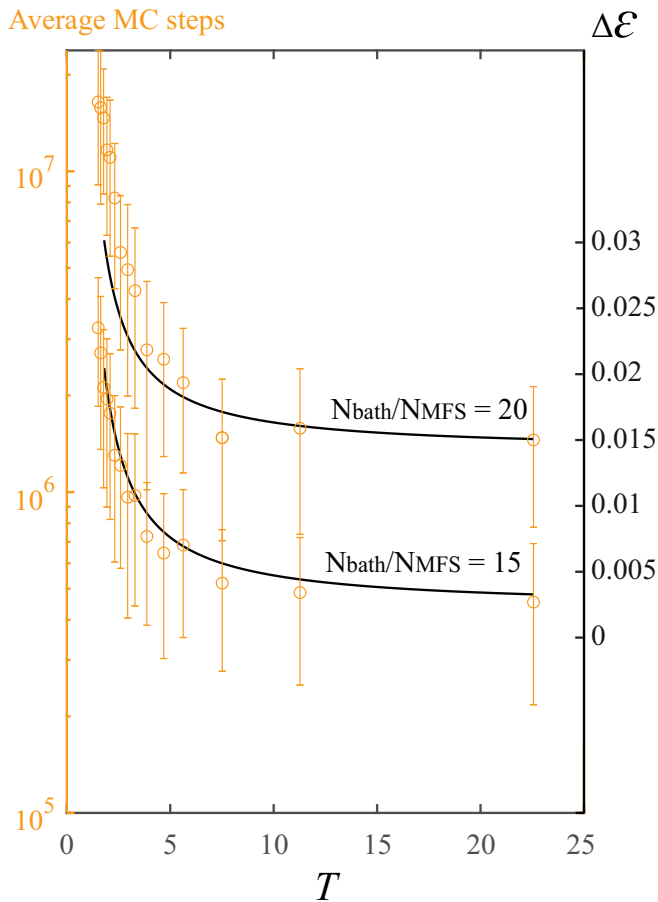
FIG. 4. The relationships between metastable state lifetime τ and energy barrier $\Delta\varepsilon$ versus the initial temperature T when $N_{bath}/N = 15$ and $= 20$. τ is measured by 150 independent simulations and marked as discrete yellow circle markers (mean values) with vertical error bars. $\Delta\varepsilon$ from the theoretical calculation is shown as continuous solid black line. The left ordinate represents the MC step and is given on a logarithmic scale. While the right ordinate represents energy and is exhibited as a linear scale. According to Eq. (5), τ and $\Delta\varepsilon$ should be overlapped.

black line. According to Eq. (5), the MC steps and $\Delta\varepsilon$ can be overlapped when the simulation results and the theoretical values are exhibited in the log scale and linear scale, respectively.

As shown in Fig. 4, a smaller reservoir will be heated to a higher temperature by a MFS with a given initial temperature. As a consequence, a moderate decrease of the reservoir size leads to smaller energy barriers and thus significantly reduce the phase transition time.

IV. SUMMARY

In summary, we have shown that the non-Markovian ME naturally appears in the mean-field system using microcanonical MC simulation. Specifically, by simulating thermal contact between a large thermal reservoir with the MFSs with different initial temperatures, it takes less time for the initial hotter system to finish the first-order paramagnetic-ferromagnetic phase transition. The occurrence of the ME here is a result of the back-reaction of the system on the reservoir, which is thus an embodiment of the non-Markovianness. Although two MFSs with different initial temperatures cool along the same route, the initial hotter MFS heats the finite 0 K reservoir more than the initial cooler one, and consequently, the free-energy barrier is reduced and less time is spent in the metastable state. In addition, our results also indicate that such strong effect survives in the thermodynamic limit. That is, although the transition time increases with the size of the full system, the rate of increase varies for the systems initialled at different temperatures. We have also discussed the effects of the size of the reservoir on the ME: A smaller reservoir yields a smaller energy barrier and consequently a faster transition.

Compared with previous "Markovian Mpemba effect" studies in nonwater substances [15,16], it is not necessary to choose the initial condition delicately in our model. Apparently, the ME emerges in any two MFSs initialled at different temperatures. Moreover, instead of just focusing on the cooling rate as in previous studies [16,18,19,34], our work embodies a phase transition, i.e., from paramagnetic to ferromagnetic, during the relaxation process, which highly resembles the water freezing in the original Mpemba experiment [1]. From this perspective, we have provided a general theoretical non-Markovian ME framework. This is enough to expand the understanding of the ME. Generally, discovering the explicit cause of the ME in water freezing is still a puzzling open problem. In the relaxation process of water, the metastable state is manifestly present, such as supercooled water, and hence the ME in water might be related to the mechanism described in this paper.

[1] E. B. Mpemba and D. G. Osborne, Phys. Educ. **4**, 172 (1969).

[2] M. Jeng, Am. J. Phys. **74**, 514 (2006).

[3] J. D. Brownridge, Am. J. Phys. **79**, 78 (2011).

[4] H. C. Burridge and P. F. Linden, Sci. Rep. **6**, 37665 (2016).

[5] G. S. Kell, Am. J. Phys. **37**, 564 (1969).

[6] I. Firth, Phys. Educ. **6**, 32 (1971).

[7] M. Vynnycky, S. L. Mitchell, and N. Maeno, Heat Mass Transf. **47**, 863 (2011).

[8] E. Deeson, Phys. Educ. **6**, 42 (1971).

[9] R. T. Ibekwe and J. P. Cullerne, Phys. Educ. **51**, 025011 (2016).

[10] P. K. Maciejewski, J. Heat Transf. **118**, 65 (1996).

[11] M. Freeman, Phys. Educ. **14**, 417 (1979).

[12] J. I. Katz, Am. J. Phys. **77**, 27 (2009).

[13] B. Wojciechowski, I. Owczarek, and G. Bednarz, Crystal Res. Technol. **23**, 843 (1988).

[14] X. Zhang, Y. Huang, Z. Ma, Y. Zhou, J. Zhou, W. Zheng, Q. Jiang, and C. Q. Sun, Phys. Chem. Chem. Phys. **16**, 22995 (2014).

[15] Z. Lu and O. Raz, Proc. Natl. Acad. Sci. USA **114**, 5083 (2017).

[16] I. Klich, O. Raz, O. Hirschberg, and M. Vucelja, Phys. Rev. X **9**, 021060 (2019).

[17] P. A. Greaney, G. Lani, G. Cicero, and J. C. Grossman, Metal. Mater. Trans. A **42**, 3907 (2011).

[18] M. Baity-Jesi, E. Calore, A. Cruz, L. A. Fernandez, J. M. Gil-Narvión, A. Gordillo-Guerrero, D. Iñiguez, A. Lasanta, A. Maiorano, E. Marinari *et al.*, Proc. Natl. Acad. Sci. USA **116**, 15350 (2019).

[19] A. Lasanta, F. Vega Reyes, A. Prados, and A. Santos, Phys. Rev. Lett. **119**, 148001 (2017).

[20] Z.-Y. Yang and J.-X. Hou, Eur. Phys. J. B **92**, 170 (2019).

[21] Z.-Y. Yang and J.-X. Hou, Mod. Phys. Lett. B **33**, 1950072 (2019).

[22] J.-X. Hou and X.-C. Yu, Mod. Phys. Lett. B **32**, 1850053 (2018).

[23] J.-X. Hou, X.-C. Yu, and J.-M. Hou, Int. J. Theor. Phys. **55**, 3923 (2016).

[24] See Supplemental Material at http://link.aps.org/supplemental/10.1103/PhysRevE.101.052106 for additional information, which includes Refs. [25–27].

[25] M. Kac, G. E. Uhlenbeck, and P. C. Hemmer, J. Math. Phys. **4**, 216 (1963).

[26] A. Vulpiani, F. Cecconi, M. Cencini, A. Puglisi, and D. Vergni (Eds.), *Large Deviations in Physics* (Springer, Berlin, 2014).

[27] A. Campa, T. Dauxois, and S. Ruffo, Phys. Rep. **480**, 57 (2009).

[28] M. Creutz, Phys. Rev. Lett. **69**, 1002 (1992).

[29] A. Gal and O. Raz, Phys. Rev. Lett. **124**, 060602 (2020).

[30] D. Mukamel, S. Ruffo, and N. Schreiber, Phys. Rev. Lett. **95**, 240604 (2005).

[31] J.-X. Hou, Phys. Rev. E **99**, 052114 (2019).

[32] P. de Buyl, G. De Ninno, D. Fanelli, C. Nardini, A. Patelli, F. Piazza, and Y. Y. Yamaguchi, Phys. Rev. E **87**, 042110 (2013).

[33] Y. Levin, R. Pakter, F. B. Rizzato, T. N. Teles, and F. P. Benetti, Phys. Rep. **535**, 1 (2014).

[34] Y.-H. Ahn, H. Kang, D.-Y. Koh, and H. Lee, Kor. J. Chem. Eng. **33**, 1903 (2016).